ELSEVIER

Biophysical Chemistry 101–102 (2002) 461–473

Biophysical Chemistry

www.elsevier.com/locate/bpc

Electrostatic free energy of the DNA double helix in counterion condensation theory

Gerald S. Manning*

Department of Chemistry, Rutgers University, 610 Taylor Road, Piscataway, NJ 08854-8087, USA

Abstract

Polyelectrolyte theory based on counterion condensation is extended from the standard line charge model to helical and double helical charge arrays. The number of condensed counterions turns out to be the same as for a line charge with charge density equal to the axial charge density of the helix. Also, the logarithmic salt dependence of the electrostatic free energy is the same in the range of lower salt concentration, so that the limiting laws remain unchanged. However, the internal free energy of the condensed layer of counterions and the overall electrostatic free energy depend on the helical parameters. At higher salt, the free energies of both single and double helix are negative, indicating electrostatic stabilization of the helical charge lattices due to the mixing entropy of the condensed counterions. Except at very low salt, the free energy of a single helix is higher than the free energy of a double helix with twice the charge density. With *B*-DNA parameters and single strands modeled as single helices, the predicted salt dependence of the free energy of transition from double helix to separated single strands has a maximum at approximately 0.2 M salt, close to the location in the laboratory of this well-known feature of the DNA strand separation transition. We also calculate the electrostatic free energy for the transition of the DNA double helix from the *B* to the *A* conformation. The *B* form is electrostatically stable over most of the salt range, but there is a spontaneous electrostatic transition to *A* near 1 M salt. The electrostatic free energy values are close to the experimental values of the overall (electrostatic plus non-electrostatic) transition free energies for *A*-philic base pair sequences. We are led to suggest that the experimentally observed *B*-to-*A* transition for *A*-philic sequences near 1 M salt in water is governed by the polyelectrolyte properties of these two conformations of the DNA double helix. The effect of ethanol, however, cannot be attributed to lowering of the bulk dielectric constant.

Keywords: Double helix; DNA; Counterion condensation theory; Free energy

*Fax: +1 732 445 5312.
E-mail address: gmanning@rutchem.rutgers.edu (G.S. Manning).

0301-4622/02/$ - see front matter
PII: S0301-4622(02)00162-X

1. Introduction

We have embarked on a project aimed at generalizing the counterion condensation theory of polyelectrolytes from its traditional underlying polyion model of a line of discrete charged sites to helical geometries that are more realistic for polynucleic acids. In an initial paper, we were able to calculate the number of condensed counterions, their internal free energy, and the total polyelectrolyte free energy of an array of charges uniformly spaced along a single helical path [1]. From these results, it is clear that our extensions of condensation theory will not change many of the essential features of the line-based theory. Specifically, a critical linear charge density for emergence of a condensed layer remains, and its value is the same as in line charge theory. Further, there will be no effect on the 'limiting laws' of line charge polyelectrolyte theory at low salt. The physical reason underlying invariance of these aspects of polyelectrolyte behavior to enhancement of structural detail is their dependence only on long-range electrostatics; the atomistic structure of the polyion is not sensed at far distances. The mathematical formulation of the extended theory, reviewed below, makes the physics transparent.

The limiting laws are derived from the small-ion concentration dependence of the polyelectrolyte free energy and are the same for helix and line charge at low salt. The free energy itself is lower for the single helix than for a line charge of the same linear charge density [1]. This result is intuitively reasonable, since the charge on the single helix may be viewed as radially dispersed from a line charge coinciding with the central axis of the helix.

Perhaps the major advantage of the extended theory will be its ability to yield an interesting concentration dependence at higher salt that differs from the line charge theory. Even at higher salt, the linear charge density critical for counterion condensation does not change, nor does the number of condensed counterions, nor does charge 'renormalization' (reduction of the effective polymer charge by exactly the amount of charge in the condensed layer of counterions [2]). But whereas the line charge polyelectrolyte free energy is positive everywhere in its salt concentration range of validity, the corresponding free energy of the single helix becomes negative at the higher end of the salt concentration range of validity (<1 M) [1]. The physical interpretation of the mathematical formulas indicates the reason. The radial dispersal of charge in the helical structure weakens electrostatic repulsions among polymer charges relative to the line model. Increasing salt weakens the repulsions in the helix still further in the range of salt where the integrity of the layer of condensed counterions is not violated. With the electrostatic repulsive component of free energy sufficiently diminished, the dominant contribution comes from the favorable local translational entropy of the condensed counterions, so the net effect is a negative free energy. The mixing entropy of the condensed counterions stabilizes the helical charge array relative to isolated charges at infinity. In the present paper, we will find other interesting trends, including some that can be checked for consistency with experimental data.

Our goal in this paper, then, is a further extension of the theory to a double helical array of charges, so that we can make applications to DNA physical chemistry. We will model both the strand separation transition of DNA and the transition between *B* and *A* conformations of the DNA double helix.

2. Theory

Associated with the transfer from bulk solution of θ counterions per charged monomer to a layer condensed on a polyion with N charged monomers is a free energy G_{transfer} referred to the product $k_{\text{B}}T$ of the Boltzmann constant and absolute temperature,

$$G_{\text{transfer}}/k_{\text{B}}T = N\theta \ln \frac{1000\theta}{\gamma \nu c Q} \tag{1}$$

In this equation, c is the salt molarity in bulk, assumed in excess over polyion charges, and γ is a bulk activity coefficient for the salt. We are thinking of a system like DNA in excess NaCl, Na_2SO_4, or $MgCl_2$, and ν in Eq. (1) is the number of counterions in the formula for the salt. The local activity of condensed counterions is θ/Q,

where Q is an internal partition function with units cm^3/mole polyion charge. It is assumed that Q does not depend on θ, which means that short-range interactions ('size effects') among condensed ions are neglected. Note that writing this equation does not commit us to the existence of a condensed layer, since θ is a variable to be determined by a free energy minimization procedure that could (and, below a threshold polyion charge density, does) require θ to vanish. An important point is that the $-\ln c$ term in G_{transfer} represents the bulk translational entropy lost when counterions condense, which in typical associating systems dictates the absence of binding in the dilute limit $c \to 0$.

A second free energy component accounts for the ionic interactions among polymer charges and small ions from the salt. In our theory, it has the form,

$$G_{\text{ion}}/k_{\text{B}}T = (1-Z\theta)^2 l_{\text{B}}\text{SUM} \tag{2}$$

where Z is the unsigned valence of the counterion, l_{B} is the Bjerrum length $q^2/Dk_{\text{B}}T$ (q is the unit electrical charge, and D is the dielectric constant of the solvent), and

$$\text{SUM} = \sum_{i<j} \frac{e^{-\kappa r_{ij}}}{r_{ij}} \tag{3}$$

where κ is the inverse Debye length, and r_{ij} is the distance between charges i and j on the polyion. This formula states that the ionic component of free energy is the sum of repulsive Debye–Hückel screened ion interactions over all pairs of charged monomers on the polyion, but with the unsigned charge on each monomer renormalized to the value $(1-Z\theta)q$. In other words, each charge on the polyion is effectively reduced by the charge of the condensed counterions.

The formula for κ^2 is $(8\pi)\times 10^{-3} N_{\text{Av}} l_{\text{B}} I$, where N_{Av} is Avogadro's number, and I is the ionic strength of the salt in molarity. The ionic strength is proportional to salt molarity c and equals it if the salt is mono: monovalent. The factor SUM in G_{ion} is thus a function of salt concentration, and in fact it diverges as $-\ln c$ in the dilute limit. It is this entropy-like divergence of the work required to charge the polyion against ionic repulsions that makes the polyion–counterion associating system unusual. The energy of dissociation becomes infinite along with the dissociation entropy, so even

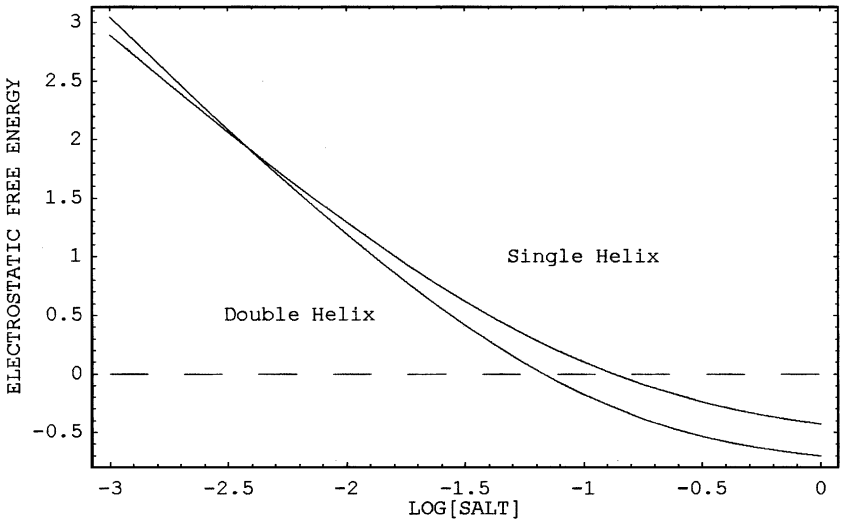

Fig. 1. The polyelectrolyte free energy of a single helix, Eq. (13), and a double helix, Eq. (19), as functions of the logarithm of uni:univalent salt molarity. Multiply the dimensionless scale by RT to get the free energy per mole monovalent charge on the polyions (per mole phosphate for DNA). The single helix is taken as one of the helices of double helical B-DNA: $a=9.225$ Å, $b=3.375$ Å, $h=5.374$ Å, $\xi=2.11$ (at 25 °C). The double helix is B-DNA: $a=9.225$ Å, $b_1=3.375$ Å, $b_2=1.688$ Å, $h=5.374$ Å, $\xi_2=4.23$, $\Delta\alpha=-3.218$ rad, $\Delta\delta=-3.696$ Å.

in dilute conditions the latter does not dominate, and counterions do not necessarily dissociate from the polyion.

For the model of a long line of N charges with uniform spacing b, all charges are equivalent, and to evaluate SUM we need only know that the distance r_n between a pair of charges separated by $n-1$ other charges along the line is equal to nb,

$$\begin{aligned}(\mathrm{SUM})_{\mathrm{line}} &= (N/b)\sum_{n=1}^{\infty}\frac{\mathrm{e}^{-\kappa nb}}{n}\\ &= -(N/b)\ln\left(1-\mathrm{e}^{-\kappa b}\right)\\ &= -(N/b)\ln\left(\kappa b\right)\\ &\quad -(N/b)\ln\frac{1-\mathrm{e}^{-\kappa b}}{\kappa b}\end{aligned} \tag{4}$$

In the second line of Eq. (4), we have noted an analytical formula for the summation in the first line. The third line isolates a leading $-\ln c$ divergent term; the second term in this line tends to zero with salt concentration c.

It is clear that the combined free energy $G_{\mathrm{transfer}}+G_{\mathrm{ion}}$ contains two functionally independent classes of terms. There are two $\ln c$ terms, one from G_{transfer} corresponding physically to the dissociation entropy of condensed counterions, and one from G_{ion} that is characteristic of the electrostatic energy in line charge geometry. The physical origin of these $\ln c$ terms is transparent. Moreover, there is no physical reason to believe that any other $\ln c$ terms lie hidden elsewhere in the free energy, for example, in the internal partition function Q (which does not contain the long-range electrostatics handled separately by the renormalized charge formulation of G_{ion}). We therefore assume that all terms in the combined free energy other than the two $\ln c$ terms are well-behaved in the low-salt limit. The two functionally independent classes of terms are then the $\ln c$ terms and the non-divergent terms.

We may now implement the equilibrium condition that the θ derivative of the combined free energy equals zero (for more detail, see Ref. [3] or [4]). The θ derivative has the form $A(\theta)\ln c + B(\theta, Q, c)$, where A and B have the indicated dependencies, and B is well-behaved in the low-salt limit. The only way such an expression can be made to vanish as an identity in c, for small c as well as large, is by removing the logarithmic divergence, $A=0$. But setting $A=0$ in the equilibrium condition $A\ln c+B=0$ leaves us with $B=0$ also. The two equations $A=B=0$ can be solved for the number of condensed counterions θ and also the internal partition function Q of the condensed layer. (The result for the former is determined entirely by the divergence, that is, we solve $A(\theta)=0$ for the equilibrium value of θ, which therefore turns out to be independent of salt concentration c). There is a threshold charge density evaluated in terms of the dimensionless charge density parameter ξ,

$$\xi = l_{\mathrm{B}}/b = q^2/Dk_{\mathrm{B}}Tb \tag{5}$$

When $\xi<1/Z$, there are no condensed counterions (the minimizing value of θ is zero), and Q is undefined. When $\xi>1/Z$, the well-known solution for the line charge model is [3,4],

$$\theta = Z^{-1}\left(1-\frac{1}{Z\xi}\right) \tag{6}$$

$$\begin{aligned}Q_{\mathrm{line}} &= 4\pi e N_{\mathrm{Av}} b^3 Z'\frac{\nu+\nu'}{\gamma v}\\ &\quad\times\left(\xi-\frac{1}{Z}\right)\left(\frac{1-\mathrm{e}^{-\kappa b}}{\kappa b}\right)^2\end{aligned} \tag{7}$$

We have not placed a subscript 'line' on θ, since it turns out that the same formula applies to both the single and double helical models. Symbols in the formula for Q_{line} thus far undefined are the base e of natural logarithms, and the coion valence Z' and number of coions ν' in the chemical formula for the salt.

To get the optimized total polyelectrolyte free energy per charged monomer G_{line}/N, that is, the reversible work required to assemble the N charges on the line from their isolated reference state at infinity, substitute the above formulas for θ and Q into the sum of the free energy components G_{ion} and G_{tansfer},

$$\begin{aligned}G_{\mathrm{line}}/Nk_{\mathrm{B}}T &= -\frac{1}{Z}\left(2-\frac{1}{Z\xi}\right)\ln\left(1-\mathrm{e}^{-\kappa b}\right)-\frac{1}{Z}\\ &\quad+\frac{1}{Z^2\xi}\end{aligned} \tag{8}$$

Turning now to the model of a single helical

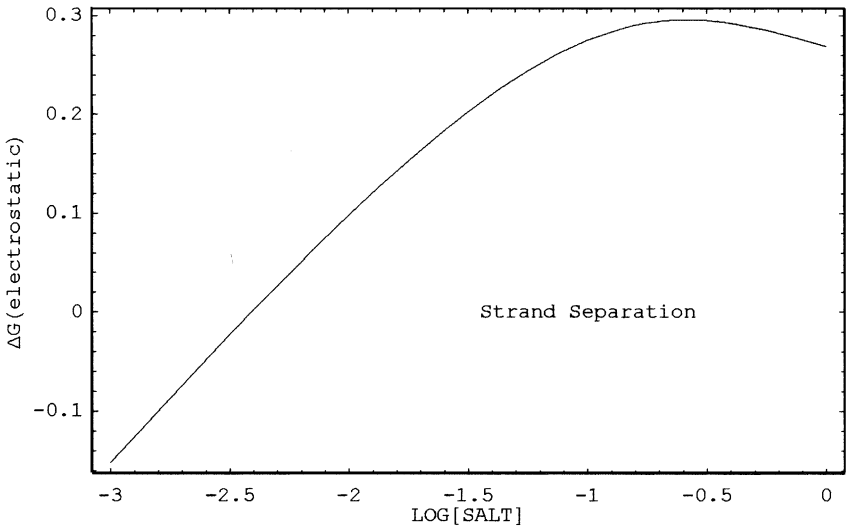

Fig. 2. The polyelectrolyte free energy component for the strand separation transition of *B*-DNA as a function of the log of uni:univalent salt molarity. Multiply the dimensionless scale by 2*RT* to get free energy per mole base pair. The separated strands are modeled as regular helices, each congruent with one of the helices in the *B*-DNA structure.

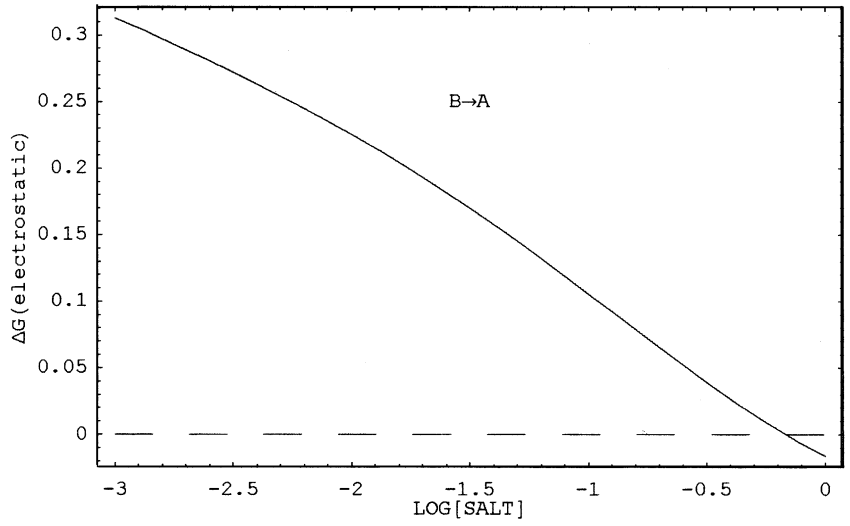

Fig. 3. The polyelectrolyte free energy component for the *B*-DNA→*A*-DNA double helical transition as a function of the log of uni:univalent salt molarity. Multiply the dimensionless scale by 2*RT* to get free energy per mole base pair. The structural parameters for *B*-DNA are given in the caption to Fig. 2. For *A*-DNA they are: $a=8.590$ Å, $b_1=2.548$ Å, $b_2=1.274$ Å, $h=4.462$ Å, $\xi_2=5.60$, $\Delta\alpha=-2.412$ rad, $\Delta\delta=8.270$ Å.

array of N charges [1], we again note that all charged sites are equivalent for a long helix, so the requirement for evaluation of SUM in Eq. (3) is knowledge of the length r_n of the chord between a pair of charge sites separated by $n-1$ other sites along the helical trajectory,

$$r_n = nb\left\{1+\left(2a^2/n^2b^2\right)\left[1-\cos(nb/h)\right]\right\}^{1/2} \qquad (9)$$

where a is the radius of the helix, and h is its rise (increment of axial coordinate per radian change of rotation angle). The length b is also present in this formula. It is essentially the same b that appears as the charge spacing in the line charge model, but here it is the uniform spacing of the projections onto the central axis of the charge sites on the helix. In other words, q/b is the linear charge density of the helix.

When Eq. (9) is used for r_n in Eq. (3), the $-\ln c$ divergence in SUM can be isolated by adding and subtracting a line charge summation (see first line of Eq. (4)),

$$(\mathrm{SUM})_{\text{Single helix}} = (\mathrm{SUM})_{\text{line}} + N\sum_{n=1}^{\infty}\left(\frac{\mathrm{e}^{-\kappa r_n}}{r_n} - \frac{\mathrm{e}^{-\kappa nb}}{nb}\right) \quad (10)$$

The logarithmic divergence is contained in $(\mathrm{SUM})_{\text{line}}$ (third line of Eq. (4)); while the explicit infinite series in Eq. (10) converges as κ (i.e. c) tends to zero, since with Eq. (9) for r_n the general term is of order n^{-3}.

The same minimization procedure employed for the line charge goes over to the single helix, and the identical number of counterions, Eq. (6), condenses on the helix, since the divergent term is identical for both models. The internal partition function of the helix is different,

$$Q_{\text{Single helix}} = Q_{\text{line}}\exp[-2(\mathrm{STRUCTURE})_{\text{Single helix}}] \quad (11)$$

where Q_{line} is given by Eq. (7), and the 'structure factor' is a convergent infinite series,

$$(\mathrm{STRUCTURE})_{\text{Single helix}} = \sum_{n=1}^{\infty}\frac{1}{n} \times\left\{\frac{\exp\left[-\kappa nb\sqrt{1+\frac{2a^2}{n^2b^2}\left(1-\cos\left(\frac{nb}{h}\right)\right)}\right]}{\sqrt{1+\frac{2a^2}{n^2b^2}\left(1-\cos\left(\frac{nb}{h}\right)\right)}} - \exp(-\kappa nb)\right\} \quad (12)$$

carrying the information that the polyion charges are arrayed along a helix of radius a and rise h. Notice from Eq. (12) that the 'structure' is relative to a line charge with the same linear charge density b^{-1} as the helix, and that $(\mathrm{STRUCTURE})_{\text{Single helix}}$ collapses to zero if the helical radius a vanishes.

The polyelectrolyte free energy of a single helix with $N=P$ charges is obtained by using Eq. (6), Eq. (11), and Eq. (12) in the formulas for G_{transfer} and G_{ion}, Eq. (1) and Eq. (2). It differs from the free energy G_{line}, Eq. (8), of a line with the same number of charges (and the same linear charge density) by a term dependent on the relative structure,

$$G_{\text{Single helix}}/Pk_{\mathrm{B}}T = G_{\text{line}}/Pk_{\mathrm{B}}T + \frac{1}{Z}\left(2-\frac{1}{Z\xi}\right)(\mathrm{STRUCTURE})_{\text{Single helix}} \quad (13)$$

The free energy of the DNA double helix is enriched by the interaction of the charges (phosphate groups) on one helix with those on the other. We assume that the monovalent negative charges of DNA are located on its phosphorous atoms, and that there are P of them on each DNA strand. The total number of DNA charges is then $N=2P$. For ideal DNA, the phosphorous atoms on each strand lie equally spaced along a right-handed helix. One helix can be geometrically transformed into the other by a screw rotation (a rotation combined with a displacement along the central axis). The crystallographic data [5] are presented such that the following representation of the two helices, $r(\phi)$ and $r'(\phi)$ is natural,

$$r(\phi) = [a\cos(\phi+\alpha), a\sin(\phi+\alpha), h\phi+\delta]$$
$$r'(\phi) = [a\cos(\phi+\alpha'), a\sin(\phi+\alpha'), h\phi+\delta'] \quad (14)$$

Notice that the helices are congruent (same radius a and rise h), and that they share the same parameter, the rotation angle ϕ. The phase angles α and α', and the vertical displacements δ and δ', have definite numerical values as given in crystallographic tables [5], and these values are different for different DNA conformations, such as the ideal A and B forms.

The linear charge density continues to be a key parameter. Appearing in the formulas below will be b_l, the uniform spacing of the projections onto the central axis of the charges on one of the helices in the duplex. The associated reduced linear charge density is $\xi_1 = l_B/b_1$. Also appearing is b_2, defined as equal to $(1/2)b_1$. The quantity b_2 is the uniform spacing of a line of $2P$ charges with the same length as the central axis of the double helix. This hypothetical line has a charge density equal to the average linear charge density of the double helix. The corresponding reduced linear charge density $\xi_2 = l_B/b_2 = 2\xi_1$.

In evaluating SUM in Eq. (3), we first make the obvious remark that the *ij* phosphate pair can either be on the same helix, or *i* can be on one helix and *j* on the other. Decomposing SUM accordingly, we get a sum corresponding to pairs of phosphates, both members of the pair residing on the unprimed helix, and another sum corresponding to pairs of phosphates with both on the primed helix. These sums are identical, and each is equal to $(\mathrm{SUM})_{\text{Single helix}}$ given by Eq. (10) with $N = P$ and $b = b_1$.

In addition to the intrahelical sums, SUM contains a summation of pairwise interactions of phosphate charges on different helical strands, and we direct attention to the evaluation of this term. From Eq. (14), we obtain an expression for the distance $r_{0n'}$ between charge site 0 located at $\phi = 0$ on the unprimed helix $r(\phi)$ and the nth charge site $\phi = \phi_n$ on the primed helix $r'(\phi)$,

$$r_{0n'} = \left\{ (nb_1 + \Delta\delta)^2 + 2a^2\left[1 - \cos\left(\frac{nb_1}{h} + \Delta\alpha\right)\right]\right\}^{1/2}$$
$$= nb_1\left\{\left(1 + \frac{\Delta\delta}{nb_1}\right)^2 + \frac{2a^2}{n^2b_1^2} \times \left[1 - \cos\left(\frac{nb_1}{h} + \Delta\alpha\right)\right]\right\}^{1/2} \quad (15)$$

where $\Delta\alpha = \alpha' - \alpha$ and $\Delta\delta = \delta' - \delta$. In writing this formula, we have used the geometric relation $\phi_n = nb_1/h$. In Eq. (15), we may take $n = 1, 2, 3, \ldots$ so that $r_{0n'}$ is the length of the chord from charge site 0 on the unprimed helix to site n 'above' on the primed helix. For the chord from site 0 to site n 'below', we again take $n = 1, 2, 3, \ldots$ while changing n to $-n$ in the first line of Eq. (15),

$$r_{0,-n'} = nb_1\left\{\left(1 - \frac{\Delta\delta}{nb_1}\right)^2 + \frac{2a^2}{n^2b_1^2} \times \left[1 - \cos\left(\frac{nb_1}{h} - \Delta\alpha\right)\right]\right\}^{1/2} \quad (16)$$

Finally, $r_{00'}$ is obtained from either Eq. (15) or Eq. (16) by setting $n = 0$, and the term in SUM corresponding to it is subsequently handled in isolation from the others. In all of these chord lengths, there is nothing special about site 0 on the unprimed helix. It can be any of the P charges on the unprimed helix, and for this reason the constituent summations in SUM all have a prefactor P.

We have at this point analyzed SUM in Eq. (3) into four separate summations (plus the isolated $00'$ term), namely, the two identical sums of pairwise interactions among charges on each of the two helical strands, the 'upward' sum of interactions between a charge on the unprimed helix and charges 'above' it on the primed helix, and the 'downward' sum of interactions between a charge on the unprimed helix and charges 'below' it on the primed helix. Each of these four sums goes from $n = 1$ to ∞, and each is either identical or similar to $(\mathrm{SUM})_{\text{Single helix}}$ in Eq. (10); that is, we may add and subtract a line charge summation in each of them, thus isolating in each the logarithmic singularity of the third line of Eq. (4) (with $N = P$ and $b = b_1$), and leaving an infinite series in each that converges in the dilute salt limit (identical or similar to the series appearing in Eq. (10)).

We determine the number of condensed counterions from examination of the $\ln c$ singularity. Since the total number of double helical charges N is equal to $2P$, we get a term from G_{transfer} in Eq. (1) equal to $-2P\theta \ln c$. Referring to the above discussion, and recalling that κ scales like $\sqrt{c}$ we get from G_{ion} in Eq. (2) the term $-2P(1 - Z\theta)^2\xi_1 \ln c$. Combining these terms, differentiating with respect to the number θ of condensed coun-

terions per charge on the double helix ($2P$ of them), and solving for θ by setting the coefficient of $\ln c$ equal to zero, we find,

$$\theta = Z^{-1}\left(1-\frac{1}{2Z\xi_1}\right) = Z^{-1}\left(1-\frac{1}{Z\xi_2}\right) \tag{17}$$

exactly the same as the classical line charge condensation formula, Eq. (6), since ξ_2 is the average linear charge density of the double helix.

Pursuing the standard minimization procedure, we arrive at a formula for the condensed layer partition function,

$$Q_{\text{Double helix}} = Q_{\text{line}}\left(\frac{1-e^{-\kappa b_1}}{1-e^{-\kappa b_2}}\right)^2 \times \exp[-2(\text{STRUCTURE})_{\text{Double helix}}] \tag{18}$$

where Q_{line} comes from Eq. (7) with $b=b_2$ and $\xi=\xi_2$. In Eq. (18) Q_{line} is thus the internal partition function of the counterions condensed on a line charge of density equal to the linear charge density of the double helix. The formula for the 'structure factor' is given below.

The polyelectrolyte free energy per double helical charge can be written in the form,

$$\frac{G_{\text{Double helix}}}{2Pk_BT} = \frac{G_{\text{line}}}{2Pk_BT} - \frac{1}{Z}\left(2-\frac{1}{Z\xi_2}\right)\ln\frac{1-e^{-\kappa b_1}}{1-e^{-\kappa b_2}} + \frac{1}{Z}\left(2-\frac{1}{Z\xi_2}\right)(\text{STRUCTURE})_{\text{Double helix}} \tag{19}$$

where G_{line} is from Eq. (8) with $N=2P$, $b=b_2$, and $\xi=\xi_2$. Accordingly, G_{line} is the polyelectrolyte free energy of a line of charges with charge density equal to the linear charge density of the double helix.

The information that the polyion is a double helix is contained in the factor $(\text{STRUCTURE})_{\text{Double helix}}$, which appears in both Eq. (18) and Eq. (19). It may be expressed as follows,

$$(\text{STRUCTURE})_{\text{Double helix}} = S_0 + S_1 + S_+ + S_- \tag{20}$$

Here,

$$S_0 = \frac{1}{2}\left(b_2/r_{00'}\right)e^{-\kappa r_{00'}} \tag{21}$$

where $r_{00'}$ is the length of the chord from a charged site on the unprimed helix to the site 'directly across' from it on the primed helix. It is obtained by setting $n=0$ in either Eq. (15) or Eq. (16). The term S_1 is an infinite series,

$$S_1 = \frac{1}{2}\sum_{n=1}^{\infty}\frac{1}{n}\left[\frac{e^{-\kappa r_n}}{\left(r_n/nb_1\right)} - e^{-n\kappa b_1}\right] \tag{22}$$

where r_n is the chord-distance between two charge sites on the same helix separated by $n-1$ other sites on that helix. This length is found from Eq. (9) with $b=b_1$. The terms S_+ and S_- both originate from the interstrand interactions,

$$S_+ = \frac{1}{4}\sum_{n=1}^{\infty}\frac{1}{n}\left[\frac{e^{-\kappa r_{0n'}}}{\left(r_{0n'}/nb_1\right)} - e^{-n\kappa b_1}\right] \tag{23}$$

and

$$S_- = \frac{1}{4}\sum_{n=1}^{\infty}\frac{1}{n}\left[\frac{e^{-\kappa r_{0,-n'}}}{\left(r_{0,-n'}/nb_1\right)} - e^{-n\kappa b_1}\right] \tag{24}$$

where $r_{0n'}$ and $r_{0,-n'}$ are interhelical chord-distances from Eq. (15) and Eq. (16), respectively. The three infinite series S_1, S_+, and S_- all converge in the limit $\kappa \to 0$. Along with the isolated term S_0, they represent the relatively short-range consequence of deforming an idealized linear lattice of charge sites into a three-dimensional double helical array.

3. Applications and discussion

3.1. Polyelectrolyte free energy

The behavior of the line charge model is simple [1]. Its polyelectrolyte free energy is nearly linear in log[salt], and lines of higher charge density have higher free energy. A line charge of charge density equal to the linear charge density of a helical charge array has a substantially higher electrostatic free energy than the helix (see, e.g. Fig. 2 of [1]). The focus of this section will be on the behavior and applications of the helical models.

We present first the polyelectrolyte free energies of single and double helices, using Eq. (13) and Eq. (19). In the graphical representation of Fig. 1, the numerical values of the double helical structural parameters are characteristic of the *B* form of DNA [5]. The structural parameters for the single helix are those of one of the helices in the double helix. Both free energies are on a 'per phosphate' basis (and in units of k_BT) and are thus directly comparable. The free energies are shown in their dependence on log[salt], where [salt] is the molarity c of uni:univalent salt such as NaCl.

Several features of the polyelectrolyte free energy stand out from Fig. 1. We begin with the monotone decrease of both curves: an increased salt concentration dampens electrostatic effects. Next, notice the linearity of both curves in the region of low salt concentration. The leading term G_{line} in both Eq. (13) and Eq. (19) is given by Eq. (8). In this equation the term that depends on salt concentration (through κ) is proportional to $-\ln(\kappa b)$ at low salt, whence the observed linearity with log[salt] at the low-salt end of Fig. 1. An important further elaboration in the range of dilute salt is that the free energy of the double helix is larger there than the free energy of the single helix. This property also follows from inspection of the leading G_{line} term for both free energies. The dominant $-\ln c$ term in Eq. (8) is multiplied by a larger numerical coefficient for the double helix than for the single helix, since the linear charge density ξ_2 for the double helix is twice as large as for the single helix. The low-salt ends of the curves in Fig. 1 are thus dominated by classical condensation line charge behavior [3]. The free energy is linear in log[salt], and is greater for the higher linear charge density.

With increasing salt concentration, the double and single helical curves cross. The polyelectrolyte free energy of the single helix becomes greater than for the double helix, despite the much higher linear charge density of the latter. Three-dimensional charge dispersal as quantitatively expressed in the STRUCTURE term is of greater degree in the double helix and seems to be the decisive factor in this salt range. (A side remark is that denaturation of a DNA double helix to single strands modeled as single helices is not implied by the crossover point, since only the polyelectrolyte contribution to the total ΔG is shown to vanish there.)

As salt concentration continues to increase, Fig. 1 shows the polyelectrolyte free energy entering a negative regime that bottoms out at $-k_BT$ per phosphate charge, or approximately -0.6 kcal/mole phosphate. The negative values signify stability of helical assemblies of identical charge sites relative to the same charges isolated at infinity. Electrostatic stabilization in this range is caused by the translational entropy of the counterions in the condensed layer [1]. The transitions to stability are in the higher salt range of the plot, but the salt concentrations there are actually modest. For the single helix the onset of electrostatic stability occurs at slightly over 0.1 M salt, while for the double helix, the threshold concentration is only approximately 0.06 M. As previously discussed [1], the mathematical condition for validity of the dominant effect of counterion condensation on free energy is that the Debye screening length κ^{-1} be much greater than the linear polyion charge spacing b, i.e. $\kappa b \ll 1$, and both nmr measurements on DNA [6] and all-atom molecular dynamics simulations [7] indicate integrity of the condensed layer for κb values as high as 0.5. The value of κb for the double helix at the stability threshold (0.063 M) is only 0.14. The electrostatic stability of helical charge arrays suggested by Fig. 1 may therefore be realistic.

Actually, we have found corroborating evidence for a negative polyelectrolyte free energy in data from computer simulations of *B*-DNA. From atomic-level molecular dynamics trajectories at moderately high counterion concentration, Jayaram et al. [8] have calculated enthalpies and entropies corresponding to bonds and angles, non-bonded van der Waal's interactions, hydration, and electrostatics including fractional charges on all atoms and DNA interactions with Na^+ counterions. From these data we have estimated the negative value -1.4 kcal/mole phosphate for the part of the free energy of *B*-DNA in water associated with phosphate charges and the Na^+ counterions. (The estimate is obtained from the column labeled 'B (water)' in the authors' Table 1(a). DNA electrostatics is said to be 'dominated by phosphate

repulsions', so the entries in rows 3 and 4 for direct electrostatic interactions among DNA atoms (unfavorable) and among counterions and DNA atoms (favorable since primarily consisting of attractive counterion–phosphate interactions) are added, and then divided by 78 to account roughly for the effect of hydration on the ionic interactions. The result is a net favorable -2.3 kcal/mole phosphate. Then the 'counterion-release' entry of row 9 is deconstructed to find the unfavorable entropic free energy of bringing free Na^+ counterions into the condensed layer. It works out, with the authors' assumptions, to $+0.9$ kcal/mole phosphate, not enough to turn around the large stabilizing contribution from direct Na^+-phosphate electrostatic energy. The stated estimate -1.4 kcal for overall favorable polyelectrolyte free energy is the sum $-2.3+0.9$ kcal.)

3.2. The strand separation transition

When *B*-form double helical DNA is heated, a narrow range of temperatures is encountered at which the constituent strands unwind from each other and separate [9]. The transition is variously called strand separation, helix-to-coil, or simply melting. Although the separated polynucleotide chains are relatively flexible, their high polyelectrolyte charge density [3] is consistent with the retention of irregular helical structure (but see below). In our application to the electrostatics of the strand separation transition, we adopt a simplified model of the single strand as a regular helix with structural parameters equal to one of the helices in intact *B*-DNA.

In Fig. 2, we plot the free energy difference,

$$\Delta g_{\mathrm{polyel}} = G_{\mathrm{Single\ helix}}/(Pk_{\mathrm{B}}T) - G_{\mathrm{Double\ helix}}/(2Pk_{\mathrm{B}}T) \qquad (25)$$

using Eq. (13) and Eq. (19). The quantity $\Delta g_{\mathrm{polyel}}$ then gives the polyelectrolyte component of the free energy of the strand separation transition in units of $k_{\mathrm{B}}T$ per phosphate (or RT per mole phosphate). To avoid confusion, note that the 'single helix' term can be multiplied and divided by 2, and then it becomes obvious that the right-hand side represents the electrostatic free energy per phosphate for the process of separation of a double helix with $2P$ phosphates into two individual strands each with P phosphates. Of course, $\Delta g_{\mathrm{polyel}}$ is just the difference of the two curves in Fig. 1, but the single differential plot in Fig. 2 provides additional insight and allows comparison with experimental data on DNA strand separation.

Over most of the range shown in Fig. 2, the electrostatic transition free energy increases with increased salt concentration; added salt stabilizes the double helix against strand separation. At lower salt, Δg is linear in log[salt]. As seen from Eq. (8), Eq. (13), and Eq. (19), the value of the slope in the linear region is the classical line charge counterion condensation value $(1/2)(\xi_1^{-1}-\xi_2^{-1})$.

The feature in Fig. 2 that is new is seen at the higher salt end of the plot. The curve begins to bend at approximately 0.1 M, hits a maximum value at 0.25 M, and then decreases. It has been known for decades, and never satisfactorily explained, that when measured values of the transition, or 'melting', temperature T_{m} are plotted against log[salt], deviation from linearity (with slope about equal to the counterion condensation predicted value) is observed in this salt range, followed by a maximum. The salt dependence of the melting temperature is strongly correlated to the salt dependence of the transition free energy, and Klump's extensive tabulation of measured overall transition free energies shows maxima at approximately 0.3 M NaCl [9]. Klump makes the interesting observation that DNA is maximally stable against disruption to individual strands in physiological salt conditions, and we can now gain from Fig. 2 an insight into this behavior as possibly a consequence of the fundamental electrostatics of helical assemblies of phosphate charges.

Modeling of the single strand as a regular helix, even if understood as simplified, is uncertain. An early energy minimization effort [10] attempted to explain the high polyelectrolyte charge density of a single polynucleotide as the net result of a locally extended chain of individual nucleotides of average length much less than characteristic of the nucleotide conformation in the double helix. There is reason to wonder, then, if a line charge with charge spacing $b_1=4.0$ Å, $\xi_1=1.8$ [3] might be a better polyelectrolyte model for the separated strand than a regular helix. We have calculated

Δg_{polyel} using the double helical model for the intact double helix and line charges for the separated strands. We continue to find a maximum (not shown), but it occurs at a salt concentration near 0.02 M, an order of magnitude less than where it is observed experimentally and predicted theoretically with the single helix model. State-of-the-art molecular dynamics simulation of a single oligonucleotide strand with variable base composition would be helpful.

3.3. The $B \rightarrow A$ transition

The DNA double helix can exist in a variety of different conformations with fully hydrogen-bonded base pairs. The *B* conformation is globally stable in aqueous solution of moderate ionic strength, including physiological, but other structures become stable in more extreme conditions. In the ideal *A* conformation the two helices are right-handed as in *B*, but the base pairs are wound near the periphery, so that a large vertical hole appears in a top view of the molecule [11]. The central hole is exposed to solvent and small ions through a gaping major groove [12]. Both the linear and three-dimensional charge density are high compared to the *B* form [8]. Interest in the *A* structure of DNA has been rekindled by high-resolution diffraction patterns showing its appearance in the DNA binding sites of some protein–DNA complexes [13]. Apparently, part of the recognition process for binding is a protein-induced $B \rightarrow A$ transition in the cognate DNA site. In this section, we present and discuss the polyelectrolyte component of the free energy of the $B \rightarrow A$ transition.

The polyelectrolyte free energy difference Δg_{polyel} for the $B \rightarrow A$ transition is plotted in Fig. 3,

$$\Delta g_{\text{polyel}} = G^{A}_{\text{Double helix}}/(2Pk_{\text{B}}T) - G^{B}_{\text{Double helix}}/(2Pk_{\text{B}}T) \quad (26)$$

where Eq. (19) is used with distinct sets of numerical values of the structural parameters of *A* and *B* forms [5]. More precisely, then, Δg_{polyel} is the polyelectrolyte component of the free energy of transition in units of *RT* per mole phosphate. The positive values seen over most of the salt range are in line with the straightforward expectation of electrostatic stability of the *B* arrangement of phosphates relative to the higher charge density *A* assembly.

Of greater interest in Fig. 3 is the electrostatic transition to negative values as the salt concentration approaches 1 M. It is known that the ease of conversion to the *A* structure is strongly dependent on the base pair sequence [14]. The *A* conformation has been observed in aqueous solution for '*A*-philic' sequences like CC·GG in and above 1 M salt but not below, while '*B*-philic' sequences like AA·TT have a stable *B* structure even in high salt [15,16]. Our polyelectrolyte theory does not refer to the base pairs at all, but only to the ionized phosphate groups. Nonetheless, the energy scale exhibited in Fig. 3 is right on target for *A*-philic sequences. The measured overall transition free energy for the CC contact under physiological conditions is 0.19 kcal/mole [14]. The electrostatic component of the transition free energy in Fig. 3 at 0.1 M salt is 0.13 kcal/mole base pair. (The number of base pairs equals the number of Ivanov 'contacts' within end effects [14]. There are two phosphates per base pair, so the values in Fig. 3 are multiplied by 2*RT*). The apparent agreement between overall and electrostatic transition free energies supports the idea discussed by Olson and Zhurkin [13] that steric clash of exocyclic base groups in the *B* conformation of *A*-philic sequences may raise the structural (non-polyelectrolyte) energy of the *B* conformer to a level more or less isoenergetic to *A*. In contrast, the structural and associated energetic characteristics of *B*-philic sequences (measured transition free energy approximately 1 kcal/mole AA·TT contact) may be such that the polyelectrolyte contribution is only a 10% perturbation on the overall large and positive free energy, not enough to induce a high-salt conformational change to *A*.

Our discussion has assumed water as solvent, and in this solvent the *B*-DNA conformation is known to be stable for all sequences in physiological salt concentration. However, the *A* form of DNA becomes stable in mixed water/alcohol solvents of sufficiently high ethanol content, and indeed, the classification into *A*-philic and *B*-philic sequences stems from the observation that the

former convert from *B* to *A* at relatively lower ethanol mole fraction [14]. Can this observation be explained in terms of our theory by using the lower bulk dielectric constants characteristic of the mixed solvents? The answer is no. We have calculated $\Delta g_{\mathrm{polyel}}$ as a function of decreasing dielectric constant at the fixed salt concentration 0.1 M (not shown), and the values are always positive (electrostatic stability of *B*). *A* more microscopic treatment of the mixed-solvent system [8] may be required for adequate accuracy.

The *A* form of DNA is usually not stable. RNA, on the other hand, is stable only in the *A* form in typical conditions, because the ribose 2′-OH group that distinguishes RNA from DNA does not fit well into a *B* structure, and possibly also because of more subtle torsion angle strains [17]. Given this circumstance, polyelectrolyte theory is not expected to contribute much knowledge toward the strong forward driving force in a hypothetical $B \rightarrow A$ RNA transition. It may be worth mentioning, however, that our results in Fig. 3 are generally consistent with simulations of an RNA sequence [17], which indicate Poisson–Boltzmann electrostatic stability of the *B* conformer, decreasing at higher salt concentrations.

In summary, our polyelectrolyte calculations provide limited but potentially useful information on the $B \rightarrow A$ transition. While implying little to nothing about the energetics of *B*-philic DNA sequences, the effect of alcohol content, or the natural preference of RNA for *A*, they raise the possibility that the polyelectrolyte contribution to the transition free energy is the controlling factor in the high salt conversion of *A*-philic sequences from *B* to *A*. The polyelectrolyte component of transition free energy in Fig. 3 favoring *B* at low salt is quantitatively similar to the measured overall transition free energy for *A*-philic sequences in the same conditions [14]. If the net contribution of other components to the transition free energy for *A*-philic sequences is small [13] and, as expected, insensitive to salt, then the high-salt conversion to *A* would be driven by the polyelectrolyte trend seen in Fig. 3. This conclusion also seems to be consistent with atomistic-level free energy simulations with Poisson–Boltzmann electrostatics [17]. The extent of decrease of the $B \rightarrow A$ transition free energy as salt is increased from 0.1 to 1.0 M is quantitatively similar there to what we see in Fig. 3, and for a particular *A*-philic sequence ‘salt is nearly able to switch the conformational preference to *A*’ [17].

Acknowledgments

Our research is supported in part by PHS Grant GM36284.

References

[1] G.S. Manning, Counterion condensation on a helical charge lattice, Macromolecules 34 (2001) 4650–4655.
[2] W. Essafi, F. Lafuma, C.E. Williams, Structural evidence of charge renormalization in semi-dilute solutions of highly charged polyelectrolytes, Eur. Phys. J. B 9 (1999) 261–266.
[3] G.S. Manning, The molecular theory of polyelectrolyte solutions with applications to the electrostatic properties of polynucleotides, Quart. Revs. Biophys. 11 (1978) 179–246.
[4] G.S. Manning, Counterion condensation theory constructed from different models, Physica A 231 (1996) 236–253.
[5] K. Aoki, S. Arnott, R. Chandrasekaran, G.A. Jeffrey, D. Moras, S. Neidle, in: W. Saenger (Ed.), Numerical Data and Functional Relationships in Science and Technology. New Series. Group VII: Biophysics, vol. 1, Nucleic Acids, Subvolume b, Crystallographic and Structural Data II, Springer, Berlin, 1989.
[6] C.F. Anderson, M.T. Record, P.A. Hart, Sodium-23 NMR studies of cation–DNA interactions, Biophys. Chem. 7 (1978) 301–316.
[7] M. Feig, B.M. Pettitt, Sodium and chloride ions as part of the DNA solvation shell, Biophys. J. 77 (1999) 1769–1781.
[8] B. Jayaram, D. Sprous, M.A. Young, D.L. Beveridge, Free energy analysis of the conformational preferences of *A* and *B* forms of DNA in solution, J. Am. Chem. Soc. 120 (1998) 10629–10633.
[9] H.H. Klump, Conformational transitions in nucleic acids, in: M.N. Jones (Ed.), Biochemical Thermodynamics, Elsevier, Amsterdam, 1988.
[10] W.K. Olson, G.S. Manning, A configurational interpretation of the axial phosphate spacing in polynucleotide helices and random coils, Biopolymers 15 (1976) 2391–2405.
[11] W. Saenger, Principles of Nucleic Acids Structure, Springer, New York, 1984.
[12] P. Langan, V.T. Forsyth, A. Mahendrasingam, D. Alexeev, S.A. Mason, W. Fuller, Complementary X-ray and neutron fibre diffraction studies of the distribution of water and cations around the *A*-DNA double helix, in:

M.U. Palma, M.B. Palma-Vittorelh, F. Parak (Eds.), Conference Proceedings of the Italian Physical Society: Water–Biomolecule Interactions, vol. 43, SIF, Bologna, 1993.

[13] W.K. Olson, V.B. Zhurkin, Modeling DNA deformations, Curr. Opin. Struct. Biol. 10 (2000) 286–297.

[14] V.I. Ivanov, L.E. Minchenkova, The A-form of DNA: in search of biological role, Mol. Biol. 28 (1995) 780–788.

[15] Y. Nishimura, C. Torigoe, M. Tsuboi, Salt induced *B*–*A* transition of poly(dG)poly(dC) and the stabilization of A form by its methylation, Nucleic Acids Res. 14 (1986) 2737–2748.

[16] Y. Wang, G.A. Thomas, W.L. Peticolas, A duplex of the oligonucleotides d(GGGGGTTTTT) and d(AAAAACCCCC) forms an *A* to *B* conformational junction in concentrated salt solutions, J. Biomol. Struct. Dynam. 6 (1989) 1177–1187.

[17] J. Srinivasan, T.E. Cheatham, P. Cieplak, P.A. Kollman, D.A. Case, Continuum solvent studies of the stability of DNA, RNA, and phosphoramidate–DNA helices, J. Am. Chem. Soc. 120 (1998) 9401–9409.